Visual Neuroscience (1999), **16**, 1037–1054. Printed in the USA.

Forebrain connections of the hamster intergeniculate leaflet: Comparison with those of ventral lateral geniculate nucleus and retina

L.P. MORIN[1,2] AND J.H. BLANCHARD[1]

[1]Department of Psychiatry, Stony Brook University, Stony Brook
[2]Program in Neurobiology and Behavior, Stony Brook University, Stony Brook

(RECEIVED December 29, 1998; ACCEPTED June 11, 1999)

Abstract

The hamster intergeniculate leaflet (IGL), part of the circadian rhythm regulatory system, has very extensive interconnections with subcortical visual nuclei. The present investigation describes IGL connections with the hamster diencephalon and telencephalon and compares them with ventral lateral geniculate nucleus (VLG) connections and retinal projections. Connections of the geniculate nuclei were evaluated using anterograde transport of iontophoretically injected *Phaseolus vulgaris* leucoagglutinin and by retrograde transport of cholera toxin β fragment. The cholera fragment was also injected intraocularly to trace retinal efferents. The IGL has ipsilateral and contralateral projections to the anterior and posterior hypothalamic nuclei, the ventral preoptic, lateral and dorsal hypothalamic areas, but not to the core ventromedial nucleus and very sparsely to the paraventricular nucleus. There are also IGL projections to the medial and lateral zona incerta, anteroventral, anterodorsal, reuniens, parataenial, paraventricular, centrolateral, central medial, and laterodorsal thalamic nuclei. IGL projections to the telencephalon are found in the horizontal limb of the diagonal band, olfactory tubercle, nucleus of the lateral olfactory tract, posterior bed nucleus of the stria terminalis, ventral pallidum, and in nuclei of the medial amygdala. The only substantial VLG projections are to bed nucleus of the stria terminalis, IGL, medial zona incerta, central medial and laterodorsal thalamic nuclei. Several of the IGL targets, the bed nucleus of the stria terminalis and zona incerta in particular, send projections back to the IGL and VLG. In addition, cells are present in the caudal cingulate cortex that project to both nuclei. Retinal projections are found in many of the regions receiving IGL innervation, including nuclei of the medial basal telencephalon, the posteromedial bed nucleus of the stria terminalis, and nuclei of the hypothalamus. A retinal projection is also visible in the lateral olfactory tract from which it extends rostrally, then medially along the base of the rhinal fissure. Fibers also extend caudally, in a superficial location, to perirhinal cortex. The results further demonstrate the widespread connections of the IGL and support the idea that the IGL modulates olfactory, photic, and circadian rhythm regulation of regulatory physiology and behavior.

Keywords: Circadian rhythm, Visual system, Anatomy, Hypothalamus, Olfactory system, Suprachiasmatic nucleus, Thalamus, Telencephalon, Light, Circadian system

Introduction

The intergeniculate leaflet (IGL) of the lateral geniculate complex was first described as a thin, retinorecipient nucleus intercalated between the dorsal lateral nucleus and the ventral lateral nucleus (VLG) in the rat (Hickey & Spear, 1976). The IGL has been shown to be a functional constituent of the circadian rhythm system [see (Morin, 1994)]. It receives bilateral, direct retinal innervation (Morin et al., 1992) and its neurons respond to photic input (Zhang & Rusak, 1989). The most prominent efferent projection of the IGL is the geniculohypothalamic tract (GHT) (Harrington et al., 1985; Card & Moore, 1989; Morin et al., 1992; Morin & Blanchard, 1995) projecting to the suprachiasmatic nucleus (SCN), site of the hypothalamic circadian clock mechanism (Klein et al., 1991).

Many of the neurons giving rise to the GHT contain neuropeptide Y (NPY). Cells containing this neuromodulator provide a good index of IGL boundaries in rats and hamsters. The IGL is now well characterized with respect to neuropeptide content of constituent neurons or afferent terminals (Harrington et al., 1985; Morin et al., 1992; Moore & Speh, 1993; Moore & Card, 1994; Morin & Blanchard, 1995), as well as the migration, development, and location of intrinsic neurons and astrocytes (Morin, 1994). Together, the various criteria identify the IGL as being quite long (about 2 mm in the hamster) with a substantial volume.

Anatomical description of the IGL has focused on its participation as part of the circadian rhythm system. Indeed, a second

Address correspondence and reprint requests to: Lawrence P. Morin, Department of Psychiatry, Health Science Center, SUNY, Stony Brook, NY 11794, USA. E-mail lmorin@epo.som.sunysb.edu

Abbreviations

AA	Anterior amygdala
ac	Anterior commissure
Aco	Anterior cortical amygdaloid N
AD	Anterodorsal thalamic N
AH	Anterior hypothalamus
AM	Anteromedial thalamic N
AOD	Anterior olfactory N, dorsal
APT	Anterior pretectal N
Arc	Arcuate N
AV	Anteroventral thalamic N
AVPO	Anteroventral preoptic area
BST	Bed N of the stria terminalis
BSTav	Bed N of the stria terminalis, anteroventral
BSTpi	Bed N of the stria terminalis, posterointermediate
BSTpl	Bed N of the stria terminalis, posterolateral
BSTpm	Bed N of the stria terminalis, posteromedial
BSTs	Bed N of the stria terminalis, suprascapular
cc	Corpus callosum
CeL	Centralamygdaloid N, lateral
Cg1	Cingulate cortex, area 1
Cg2	Cingulate cortex, area 2
CL	Central lateral thalamic N
CM	Central medial thalamic N
cp	Cerebral peduncle
CPT	Commissural pretectal area
DA	Dorsal hypothalamic area
DLG	Dorsal lateral geniculate N
DM	Dorsomedial hypothalamic N
EP	Entopeduncular N
f	Fornix
fi	Fimbria
fr	Fasciculus retroflexus
GHT	Geniculohypothalamic tract
GP	Globus pallidus
Hb	Habenula
HDB	Diagonal band of Broca, horizontal limb
IAM	Interanteromedial thalamic N
ic	Internal capsule
IGL	Intergeniculate leaflet
3	Third ventricle
IMA	Intramedullary thalmic area
IMD	Intermediodorsal thalamic N
LA	Lateroanterior hypothalamic N
LD	Laterodorsal thalamic N
LDVL	Lateral dorsal thalamic N, ventrolateral
LH	Lateral hypothalamic area
LHb	Lateral habenula
LO	Lateral orbital cortex
LOT	N lateral olfactory tract
LP	Lateral posterior thalamic N
LPO	Lateral preoptic area
LSI	Lateral septal N, intermediate
LV	Lateral ventricle
MCPO	Magnocellular preoptic N
MCPC	Magnocellular N of the posterior commissure
MD	Mediodorsal thalamic N
MDM	Mediodorsal thalamic N, medial
Me	Medial amygdala
MeA	Medial amygdaloid N, anterior
MHb	Medial habenula
MO	Medial orbital cortex
MPA	Medial preoptic area
MPN	Medial preoptic N
mt	Mammillothalamic tract
MTu	Medial tuberal N
NPY	Neuropeptide Y
oc	Optic chiasm
OPT	Olivary pretectal N
ot	Optic tract
Pa	Paraventricular hypothalamus
pc	Posterior commissure
PC	Paracentral thalamic N
Pir	Piriform cortex
PH	Posterior hypothalamic area
PHAL	*Phaseolus vulgaris* leucoagglutin
PLi	Posterior limitans N
PMV	Premammillary N, ventral
Po	Posterior thalamic group
PoMn	Posteromedian thalamic N
PrC	Precommissural N
PRh	Perirhinal cortex
PT	Parataenial thalamic N
PVA	Paraventricular thalamic N, anterior
PVP	Paraventricular thalamic N, posterior
Re	Reuniens thalamic N
RCh	Retrochiasmic area
RF	Rhinal fissure
Rh	Rhomboid thalamic N
Rt	Reticular thalamic N
SCN	Suprachiasmatic N
SG	Supragenicular thalamic N
SHy	Striohypothalamic N
SI	Substantia innominata
sm	Stria medullaris
SM	N stria medullaris
SO	Supraoptic N
SON	Supraoptic N
sPVz	Subparaventricular zone
st	Stria terminalis
SubG	Subgeniculate N
TC	Tuber cinereum
Tu	Olfactory tubercle
VL	Ventrolateral thalamic N
VLG	Ventral lateral geniculate N
VLO	Ventrolateral orbital cortex
VM	Ventral medial thalamic N
VMH	Ventromedial hypothalamic N
VP	Ventral posterior thalamic N
ZIl	Zona incerta, lateral
ZIm	Zona incerta, medial

large IGL-efferent projection is to the contralateral IGL (Morin & Blanchard, 1995). Despite the indication that the IGL reciprocally connects with the superior colliculus (Taylor et al., 1986; Morin & Blanchard, 1998), there has been little effort to discern the full extent of its ascending or descending projections. In the gerbil, anterograde tracer injections into the IGL/VLG region revealed a widespread projection pattern to hypothalamic nuclei and zona incerta (Mikkelsen, 1990). This general pattern has recently been affirmed in the rat (Horvath, 1996; Moore et al., 1996; Horvath, 1998), with the added observation that the terminal regions of IGL

efferents innervate the hypothalamus in a pattern similar to that described for rat SCN efferents (Watts et al., 1987; Horvath, 1997).

The present study is part of a general effort to provide a thorough description of the hamster IGL connections. Initial consideration of this topic has demonstrated extensive, often reciprocal, connections between the IGL and tectal or pretectal nuclei (Morin & Blanchard, 1998). In addition, such connections are frequently bilateral. The VLG connects with many of the same midbrain visual nuclei as the IGL, often reciprocally and bilaterally as well. However, the two nuclei can be distinguished by criteria of cell type [e.g., location of NPY-immunoreactive (IR) neurons], as well as of connectivity. One such criterion is that the VLG does not project to the contralateral IGL. Therefore, the present investigation was conducted to elucidate and compare projections from the IGL and VLG to the hamster forebrain. The *Phaseolus vulgaris* leucoagglutinin (PHAL) anterograde tracing method confirmed the presence of widespread forebrain projections from the IGL, but not from the VLG. Retrograde tracing methods using cholera toxin β fragment (CT-β) were used to affirm the PHAL data and the distinctions between the IGL and VLG efferent projection patterns. Also analyzed were retinal projections to rostral diencephalon and telencephalon which were compared to the patterns of IGL and VLG efferents.

Methods

Adult, outbred male golden hamsters (Charles River, Wilmington, MA) were maintained with free access to food and water under a 14-h light/10-h dark photoperiod in individual, polypropylene cages. All surgery and perfusions occurred during the light phase of the photoperiod in animals deeply anesthetized with sodium pentobarbital (Anpro Pharmaceutical, Arcadia, CA; 100 mg/kg body weight).

Surgery

Animals received injections of CT-β (1%; product #104, List Biological Labs., Inc., Campbell, CA) or *Phaseolus vulgaris* leucoagglutinin (PHAL; 2.5%) administered iontophoretically (2 μA for CT-β and 5–7 μA for PHAL pulsed 7 s ON, 7 s OFF for about 4 min). In some cases, CT-β and PHAL were injected jointly by iontophoresis according to the method of Coolen and Wood (Coolen & Wood, 1998). In these animals, the concentration of each tracer was reduced to 50% of the concentration when used alone and the stimulus parameters were 6 μA for 6–10 min. Retrograde transport of CT-β or anterograde transport of PHAL was permitted for 3–5 days. At the end of the transport period, each animal was deeply anesthetized with pentobarbital and perfused transcardially with physiological saline followed by 4% paraformaldehyde in 0.1 M phosphate buffer with sodium m-periodate and lysine added (McLean & Nakane, 1974). The five brains injected with PHAL into the IGL and two of the three that received the same treatment into the VLG for which the efferent anatomy is described were originally part of a previous study of connections with midbrain nuclei (Morin & Blanchard, 1998). The third VLG-injected brain (Case 98-17) was obtained specifically for this investigation. Areas identified, using one of the tracers, as connected to the VLG or IGL were injected in additional animals with the other tracer in order to verify the existence of such connections.

Histological procedures

Each brain was removed, postfixed for 1 h, cryoprotected in a series of sucrose solutions to 30% sucrose in phosphate buffer, then frozen and serially sectioned (30 μm) in the coronal plane. Sections were collected in 0.01 M phosphate-buffered saline with 0.05% sodium azide. All immunohistochemical reactions were performed using free-floating sections. Immunoperoxidase reactions were done using the ABC technique (Hsu et al., 1981) (Vector kit) and diaminobenzidine as the chromogen. Antisera to CT-β (goat; List Biological Labs., Inc., Campbell, CA) and PHAL (goat; Vector, Burlingame, CA or rabbit; DAKO, Carpinteria, CA) were used.

Microscopy

Brain sections from PHAL-injected animals were evaluated with a Nikon Optiphot microscope using bright- and dark-field techniques. All material reacted for PHAL-IR was specifically examined for the presence of terminal boutons among fibers of passage. The results of such inspection were utilized to decide the locations in which the CT-β retrograde label should be injected. PHAL injections label a cluster of neurons around the injection site. The volume described by the cluster was considered the region of effective label uptake (Morin & Blanchard, 1998). The center of each CT-β injection has a slightly more brilliant appearance when viewed using dark-field microscopy. It is surrounded by a region of reaction product that is distinctly denser than slightly more distal areas. As with our previous work on this topic, the volume within the boundary of this denser region is considered the zone of effective CT-β uptake. Technical issues concerning the difficulty of identifying the precise area within which the applied tracer is actually incorporated for transport by neurons have been discussed previously (Morin & Blanchard, 1998). Locations of retrogradely labeled neurons were viewed in the coronal plane and drawn on paper using a camera lucida. Coronal drawings of PHAL-IR fibers were made using a combination of the camera lucida and an inverted video monitor and associated computer. Drawings were made directly onto the screen of the video monitor using a light pen (FTG Data Systems, Stanton, CA) and CorelDraw software. Digitized photomicrographic images of tissue sections were obtained using a Sony color video camera and a Snappy image capture device. Composite images were created from the originals using Adobe Photoshop.

Results

All animals receiving IGL injections of PHAL (Fig. 1) had patterns of labeled fibers and terminals in the forebrain that were generally similar to each other, and those receiving VLG injections had patterns of PHAL-IR that were alike. However, there were differences between individuals injected in a particular nucleus with respect to the apparent density of labeled projections. For example, the density illustrated for the SCN innervation in Case 94-43 (Fig. 2E) was much less than that seen in Case 94-33 (Fig. 3B). Innervation differences between individuals may have been related to the specific injection site within the overall length of the nucleus or it may have been related to the fact that there were fewer IGL neurons filled with PHAL-IR as in Case 94-43. Table 1 summarizes the investigators' visual estimations of the density of projections to or from the IGL and VLG, and from the retina as determined from all the cases examined. Although the data are suggestive, there were insufficient cases to allow unequivocal conclusions regarding topographical organization of projections from IGL or VLG to the diencephalon.

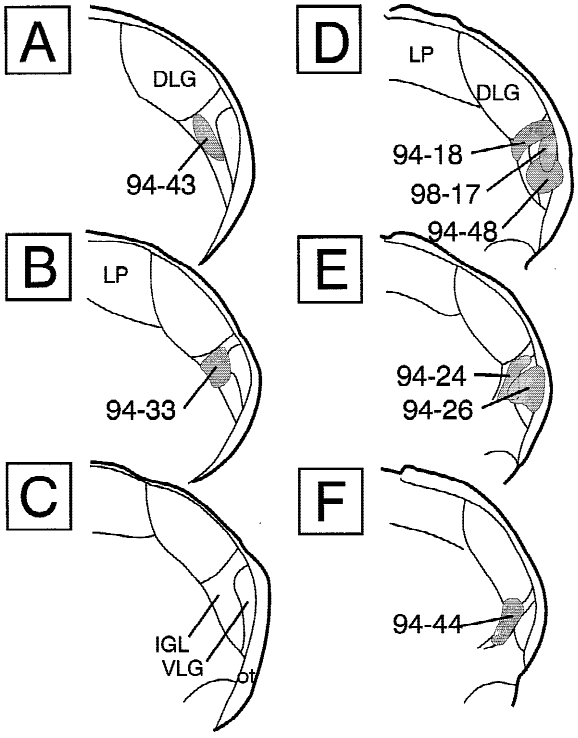

Fig. 1. Sites of PHAL iontophoretic injection into the IGL or VLG. The number of each site identifies the experimental case. As described in the Methods section, the shaded area at each site is the region of uptake by neurons determined from the locations of labeled cells.

Anterograde analysis of IGL-efferent projections

At the level of the anterior commissure (Fig. 2A), fibers and terminals are common in the horizontal limb of the diagonal band of Broca. They are scattered laterally in the olfactory tubercle, nucleus of the lateral olfactory tract, and medial nuclei of the amygdala (Figs. 2A–2I and 3A–3C).

A few fibers and terminals are also found in the ventral medial and intermediate septum and anterior divisions of the bed nucleus of the stria terminalis (Fig. 2A). Fibers and terminals are dense in the posteromedial division of the bed nucleus of the stria terminalis (Figs. 2C and 3A). A cascade of fibers spreads ventrolaterally through the ventral pallidum into anterior and medial amygdaloid areas. Fibers extend ventrally from the posterior bed nucleus with moderate density into the lateral preoptic area and lateral hypothalamus (Fig. 3A). Numerous fibers with terminals are found ventromedially in the subparaventricular zone of the anterior hypothalamus (Figs. 2C–F) and in the SCN (Figs. 2D and 2E). Note that all other cases which sustained injections further caudally than Case 94-43 (illustrated in Fig. 2) had much denser innervation to the SCN similar to that shown for Case 94-33 (Fig. 3B).

Labeled fibers with terminals are present throughout most of the hypothalamus, but are not found in the ventromedial nucleus and are sparse in the paraventricular nucleus. Terminals and fibers are also sparse throughout the ventral hypothalamus caudal to the SCN (Figs. 2G–2L and 3C). The dorsal hypothalamic area is modestly innervated (Figs. 2H and 3C) and a particularly dense terminal field is evident in the posterior hypothalamic nucleus (Figs. 2K and 2L). Modest innervation is also present in the supramammillary region (Fig. 2M).

Abundant fibers enter the dorsolateral thalamus through the posteromedial division of the bed nucleus of the stria terminalis. In rostral thalamus, there are moderate projections to the parataenial and anterior paraventricular nuclei (Figs. 2B–2D and 3A). There is innervation of the posterior paraventricular thalamus as well (Figs. 2G–2M and 3C). A particularly robust terminal plexus is present in the lateral nucleus reuniens and medial zona incerta (Figs. 2B–2G, 3B, and 3C). Innervation appears to arrive in the zona incerta through the external medullary lamina and across the ventral posterolateral thalamic nucleus (Figs. 2F–2M and 3C). As these fibers near the midline, some turn dorsally to the nucleus reuniens, but much of the reuniens innervation appears to be derived from fibers extending ventromedially between the ventral posteromedial and ventral posterolateral thalamic nuclei (Figs. 2F and 2G). The rostral appearance of such fibers is visible in Fig. 3C. Fibers and terminals form a modestly dense, continuous, bilateral U-shaped plexus in the centrolateral and paracentral thalamic nuclei (Figs. 2E, 2F, and 3B). Fibers without terminals are commonly seen traversing the laterodorsal thalamic nucleus and rostral dorsolateral geniculate nucleus toward midline pretectal structures (Figs. 2F–2H).

Contralateral IGL projections and routes of decussation

As a rule, IGL projections to ipsilateral nuclei are mimicked by similar, but much less dense, projections to the contralateral side (Fig. 2). If a terminal field is fairly sparse, as in the region of the olfactory tubercle or amygdala, the visible contralateral projections tend to be limited to a few fiber segments (Figs. 2D–2G). Midline structures such as the SCN, the thalamic central medial nucleus, and the nucleus reuniens receive innervation which is nearly bilaterally symmetrical (Fig. 2E).

Decussating pathways are evident in the supraoptic decussations, the nucleus reuniens, dorsal hypothalamic area, and central medial thalamic nucleus. An additional decussation of IGL fibers exists in the posterior commissure and has been described elsewhere (Morin & Blanchard, 1998). A clear fiber path extends from the ipsilateral dorsolateral bed nucleus of the stria terminalis, posterior division, to the same location contralaterally *via* the nucleus reuniens. It is probable that innervation of the contralateral dorsal and lateral hypothalamus arrives *via* this decussation (Fig. 2E). However, fibers in the optic chiasm also appear to exit into adjacent hypothalamus on both sides of the midline. The SCN is densely innervated bilaterally. On the ipsilateral side, numerous adjacent fibers lying in a dorsolateral-ventromedial plane are found dorsolateral and caudal to the nucleus, suggesting that much of the SCN innervation might arrive by traversing the hypothalamus from a dorsolateral point of entry. Contralaterally, the picture is much the same in and around the SCN. Although some fibers clearly enter each SCN from the supraoptic decussation, there is no certainty regarding the percentage of SCN innervation contributed from this decussation.

The dorsal hypothalamic area and posterior hypothalamic nucleus are regions of immense complexity because of the density of innervation and the confusion of efferents or afferents. Fig. 2L shows, for example, a dense terminal plexus in the posterior nucleus seeming to originate from fibers extending medially in the external medullary lamina and medial lemniscus. However, Fig. 2M indicates that many fibers are found medially, oriented vertically in the periventricular fiber system. It is not clear whether these fibers are

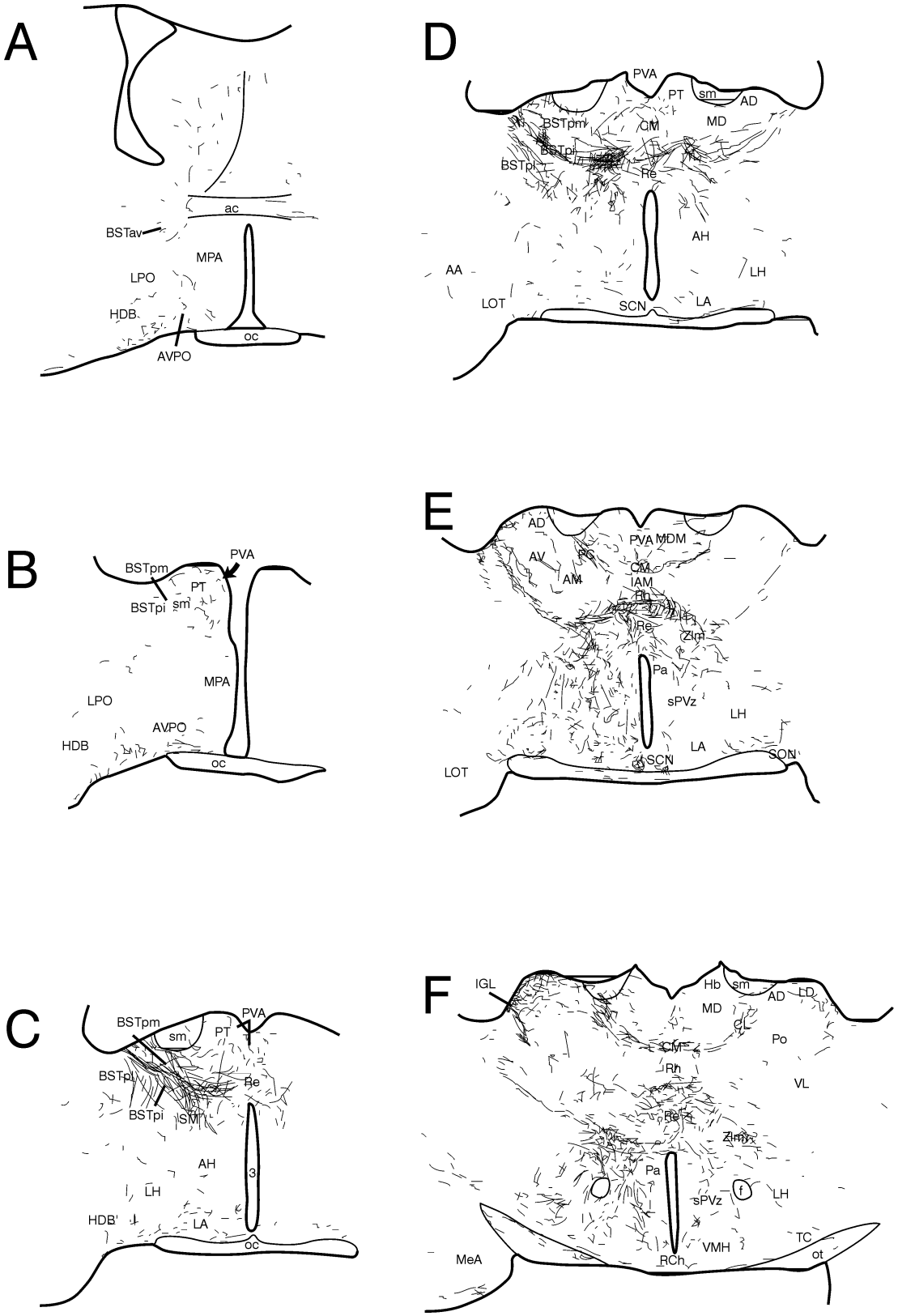

Fig. 2. Fibers and terminals in the diencephalon and basal telencephalon following iontophoretic injection of PHAL in the IGL (Case 94-43). The injection site (*) was quite well limited to the IGL. Other areas of nonspecific tracer spread (shading) are shown in levels I–M. (*Figure continues on next two pages.*)

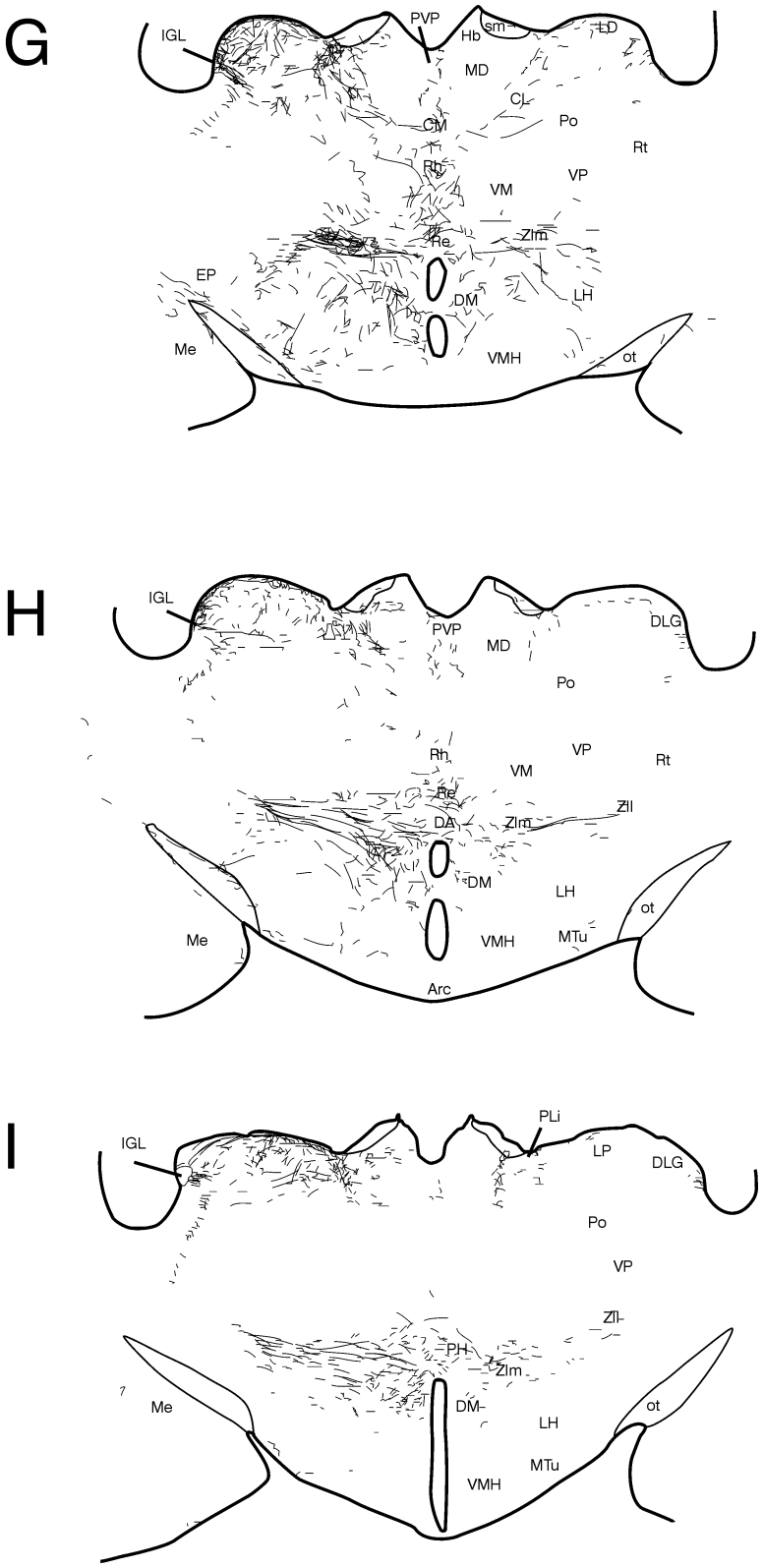

Fig. 2. (*Figure continues on next page.*)

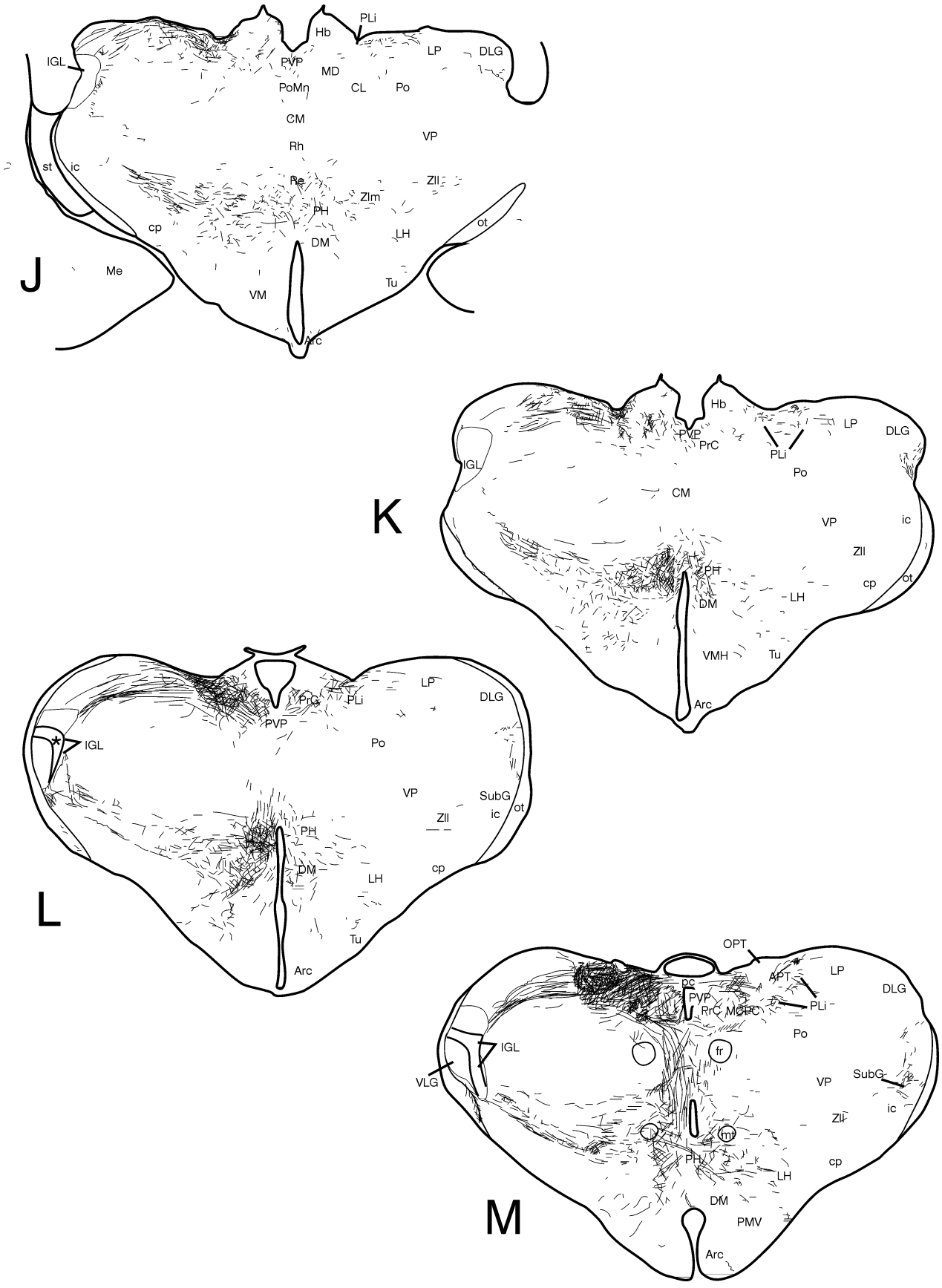
J
PLi
Hb
IGL
PVP
LP
DLG
MD
PoMn
CL
Po
CM
VP
Rh
st
ic
Re
Zll
Zlm
PH
cp
ot
DM
LH
Me
Tu
VM
Arc
K
Hb
PVP
PrC
LP
DLG
PLi
IGL
Po
CM
VP
ic
Zll
PH
cp
ot
LH
DM
VMH
Tu
Arc
L
LP
PrC
PLi
DLG
PVP
IGL
Po
VP
SubG
ic
ot
Zll
PH
DM
LH
cp
Tu
Arc
M
OPT
APT
LP
pc
DLG
PVP
PrC
MCPC
PLi
Po
IGL
fr
VLG
VP
SubG
ic
Zll
PH
LH
cp
DM
PMV
Arc

Fig. 2.

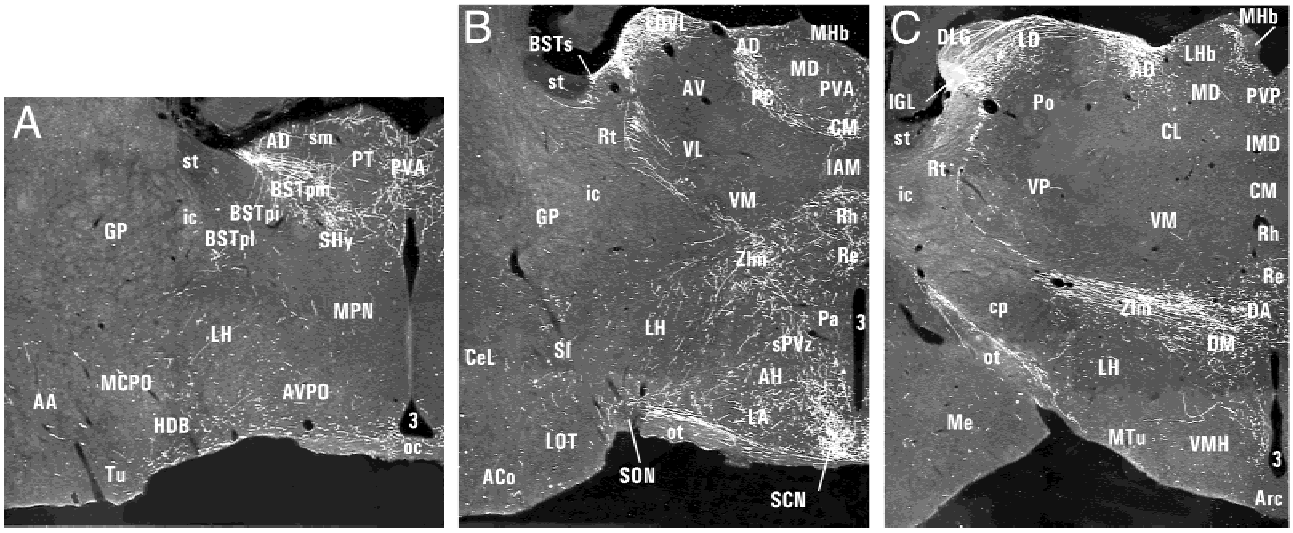

Fig. 3. Dark-field photomicrographs at (A) rostral, (B) middle, and (C) caudal hypothalamic levels showing PHAL-IR fibers following an injection of tracer into the IGL (Case 94-33). Scale bar = 500 μm.

arriving in the posterior hypothalamus from a dorsal route or are projecting dorsally to pretectal areas from a ventral route.

Anterograde analysis of VLG-efferent projections

The densest innervation of a diencephalic area by the VLG is in the intramedullary area of the lateral posterior thalamic nucleus (Figs. 4E and 4F). An extensive, moderately dense terminal field is also present in the medial and lateral zona incerta (Figs. 4C–4E). Rostrally, sparse innervation of the lateral hypothalamus and nucleus reuniens arrives *via* the posteromedial division of the bed nucleus of the stria terminalis (Figs. 4A and 4B). A few fibers are seen medially ventral to the stria medullaris with innervation evident in the central medial and centrolateral thalamic nuclei (Figs. 4A–4C). There is also sparse innervation of the posterior hypothalamic region (Figs. 4D–4F). As with the projections of the IGL, it is not possible to determine whether they arrive from a lateral location *via* the zona incerta or from a dorsal route *via* the periventricular fiber system.

Retrograde analysis of IGL- and VLG-efferent projections

Every PHAL injection into the IGL resulted in a small number of neurons outside the IGL taking up the tracer. For this reason, the retrograde label, CT-β, was applied to sites (Fig. 5) that were apparent targets of IGL or VLG neurons as determined from the PHAL-IR material. Injection of CT-β into the medial zona incerta resulted in both labeling of neurons in dorsal and medial IGL and in the VLG (Table 1; Fig. 6A). This was the only CT-β injection site that resulted in neurons being labeled ipsilaterally and contralaterally in both brain nuclei. Injection into the posterior bed nucleus of the stria terminalis (Fig. 6B) and central medial thalamic nucleus also labeled moderate numbers of neurons in both the IGL and VLG, but were bilateral only in the IGL. In contrast, injections into the anterior amygdala, septum, or parataenial nuclei labeled neurons only in the IGL, primarily on the ipsilateral side but with a few labeled contralaterally. Injections into the thalamic nucleus reuniens and several hypothalamic locations (anterior, lateral, and posterior nuclei) labeled neurons in the IGL, but not the VLG (cf. anterograde tracing data above). An injection into a very medial subparaventricular hypothalamic region (Case 98-5) labeled a few cells bilaterally in the IGL. Injections into the anterior hypothalamic nucleus, the lateral hypothalamus (Fig. 6C), and the posterior hypothalamus also labeled neurons bilaterally in the IGL. An injection of CT-β into the intramedullary area of the lateral posterior thalamic nucleus labeled numerous cells in the IGL and VLG.

IGL-afferent projections

After an injection of CT-β into the IGL, labeled neurons are evident in relatively few forebrain structures. In the telencephalon, a small but consistent collection of cells is found in the caudal cingulate cortex (Fig. 7A). PHAL injection into this region labeled fibers and terminals in the IGL. An occasional cell is evident in the medial amygdala, medial septum, and region of the olfactory tubercle. A slender group of neurons of modest number is distributed in the posterointermediate division of the bed nucleus of the stria terminalis (Fig. 7B). This set of cells extends caudomedially, becoming contiguous with the medial zona incerta where there is also a modest collection of labeled neurons (Fig. 7C). Caudally, this group is reduced in number and cells are scattered in the medial zona incerta/posterior hypothalamic area. At this level, a second group consisting of a moderately large number of cells is evident in the lateral zona incerta. Ipsilaterally, this group merges with numerous labeled neurons in the subgeniculate nucleus further laterally (Fig. 7D).

Small numbers of CT-β labeled cells are also present, as previously reported (Morin et al., 1992), around the SCN, in the anterior hypothalamus, and in the retrochiasmatic region, with an occasional cell seen in the lateral tuberal hypothalamus. Occasional neurons are also found contralaterally in the same areas. Dorsally, a few cells are present in the ventral habenula. Many more labeled neurons are found dorsally and caudally in mesencephalic nuclei of the pretectum and (Morin & Blanchard, 1998).

Table 1. *Connections of the hamster forebrain with the IGL, VLG, and retina in comparison with targets of SCN projections*[a]

	From IGL	From VLG	From retina	To IGL	To VLG	From SCN[b]
Anterior hypothalamus	++		+++	+/−		+
Anterior ventral thalamic N	+/−			−		
Anterior amygdaloid N, ventral	+		+			
Anterodorsal thalamic N	+					
Anteroventral preoptic N	++		+			+[c]
Arcuate N						+
BST, perifornical	+++	+	+	+		+
BST, posterointermediate	+++	+	+++	++	+	+
BST, posterolateral	+					
BST, anteromedial	+					+
BST, posteromedial	+	+	+			+
BST, anteroventral	+					
Central medial thalamic N	++	+	+			
Centrolateral thalamic N	++					
Cingulate cortex				++	+	
Diagonal band of Broca, horiz. limb	+					
Dorsal hypothalamic area	+		+			+
Dorsomedial hypothalamic N	+		+			+
Habenula	+			+		+
Intergeniculate leaflet	++++[d]	+[d]	+++		+++	[e]
Intramedullary thalamic area	+	+++	++			
Lateral olfactory tract N	+		+			
Lateral hypothalamus	++		++		+/−	
Lateroanterior hypothalamic N	++		++	+	+/−	+
Laterodorsal thalamic N	++	++				
Medial amygdaloid N	+		+	+/−		+
Medial preoptic area	+/−					+
Median preoptic N	+					+
Mediodorsal thalamic N						+
Olfactory tubercle	+		+	+/−		
Parataenial thalamic N	++					+
Paraventricular hypothalamic N	+/−		+/−			+
Paraventricular thalamic N, post.	+					+
Paraventricular thalamic N, ant.	+					+
Perirhinal cortex			+			
Piriform cortex	+		+			
Posterior hypothalamic N	+++			+		+
Premammillary N						+
Retrochiasmatic area	+/−			+	+/−	+
Reuniens thalamic N	+++		+/−			+
Septum, lateral intermediate	+/−					
Septum, lateral ventral						+
Septum, medial				+/−		
Subgeniculate thalamic N	++		+	+++	+++	
Subparaventricular zone	++		++			+
Suprachiasmatic N	++++		+++++			+[e]
Supramammillary N	+					+
Supraoptic N						+
Tuberal hypothalamus	+		+	+/−	+/−	+
Ventrolateral preoptic N	++		++			+
Ventromedial hypoth. N, core						
Ventromedial hypoth. N, shell	++		+			
Zona incerta, lateral	++	++	+	+++	+	
Zona incerta, medial	+++	++		++	+	

[a]Empty cell: no evident connection; +/−: very sparse; +: sparse; ++: modest; +++: moderate; ++++: dense; and +++++: extremely dense.
[b]Data from Morin et al., 1994, except for anteroventral preoptic nucleus.
[c]Hamster: Morin and Blanchard (unpublished data); rat: Watts et al., 1987.
[d]Contralateral to injection site.
[e]Innervation arises from cells around SCN.

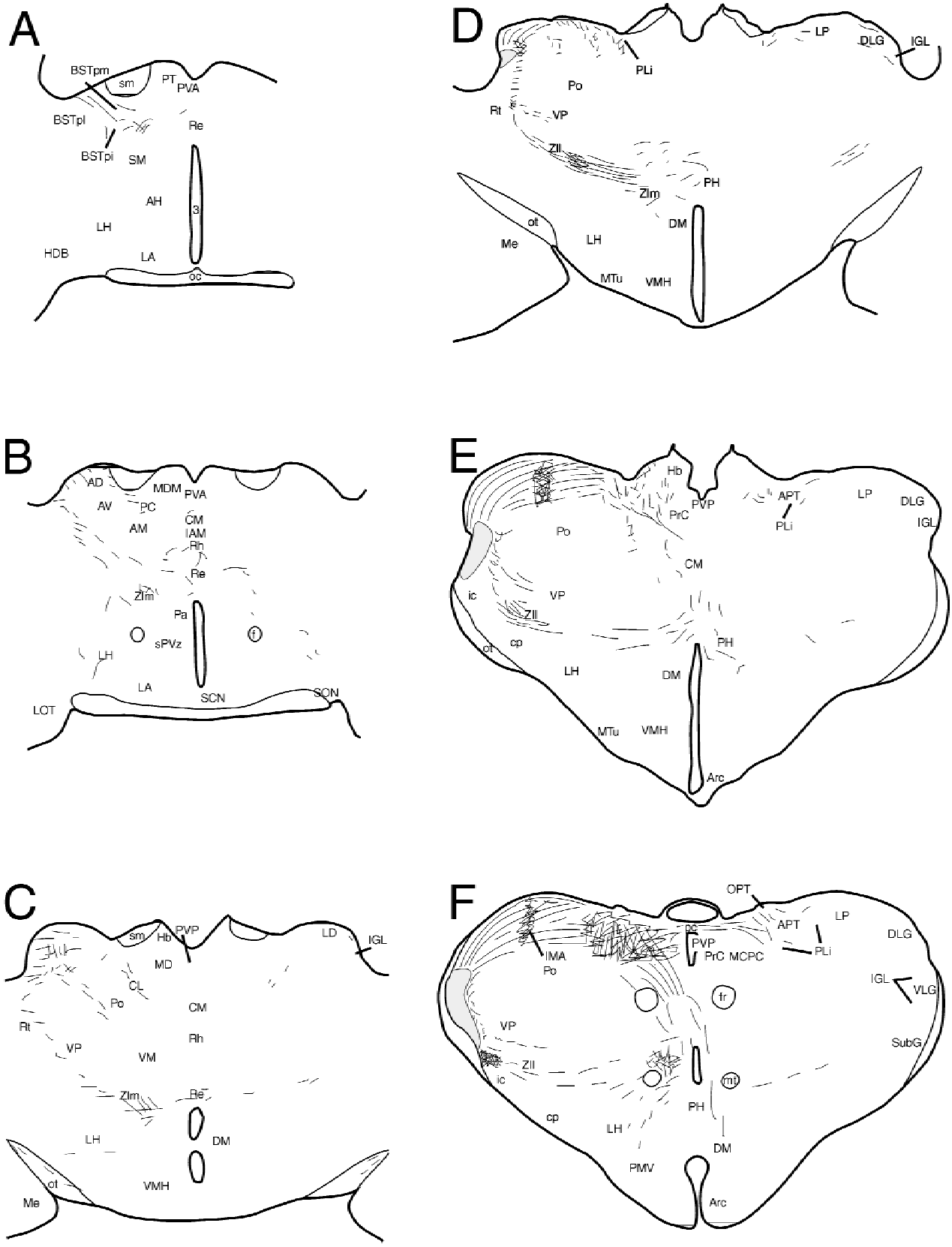

Fig. 4. Fibers and terminals in the diencephalon and basal telencephalon following iontophoretic injection of PHAL in the VLG (schematic composite based on Cases 94-26 and 94-48). The shaded areas in levels D–F indicates a region occluded by immunoreactivity to nonspecific tracer spread.

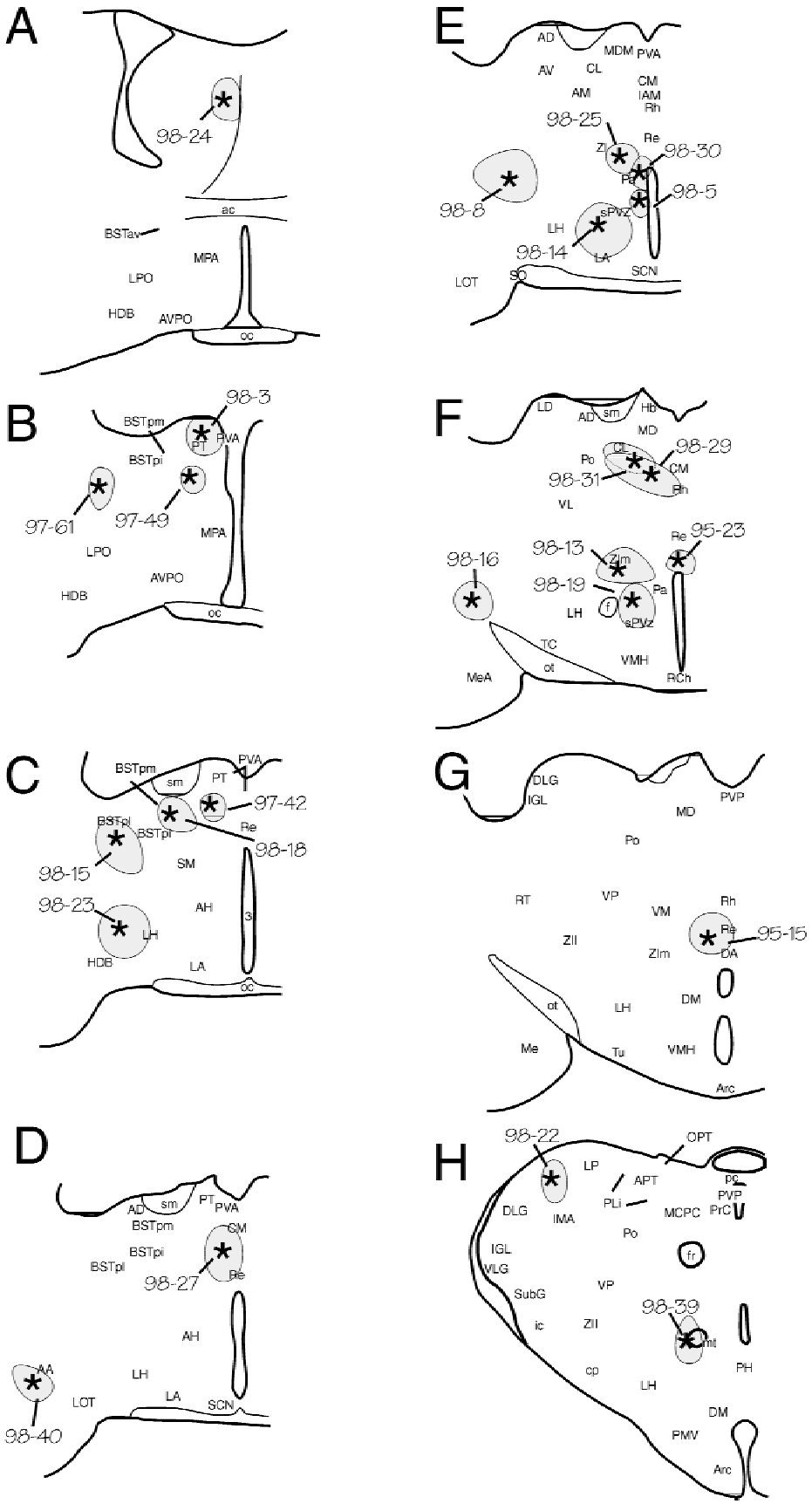

Fig. 5. Sites of iontophoretic injections of the retrograde tracer, CT-β. Asterisks indicate tip locations of the iontophoresis electrodes. The shaded region indicates the zone of effective label uptake determined as described in the Methods section. The number of each site identifies the experimental case. Most of these sites were simultaneously injected with PHAL.

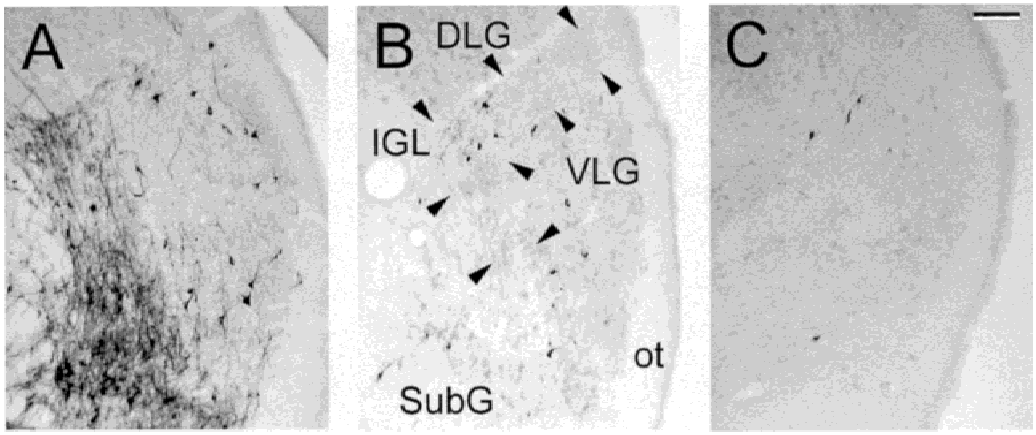

Fig. 6. CT-β-labeled neurons in the IGL following tracer injection in the (A) medial zona incerta (Case 98-13), (B) posterointermediate division of the bed nucleus of the stria terminalis (Case 98-18), and (C) far lateral hypothalamus (Case 98-16). The injection sites for these cases are shown in Figs. 4F, 4C and 4F, respectively. Scale bar = 100 μm.

VLG-afferent projections

There are few forebrain sites with neurons projecting to the VLG. The largest collections of such cells are found bilaterally in the medial and lateral zona incerta and in the subgeniculate nucleus. Neurons are also consistently seen in the posterointermediate bed nucleus of the stria terminalis and caudal cingulate cortex. Injection of PHAL into the latter area labeled fibers with terminals in the VLG. Scattered cells are also sparsely distributed in lateroanterior, retrochiasmatic, and tuberal hypothalamus.

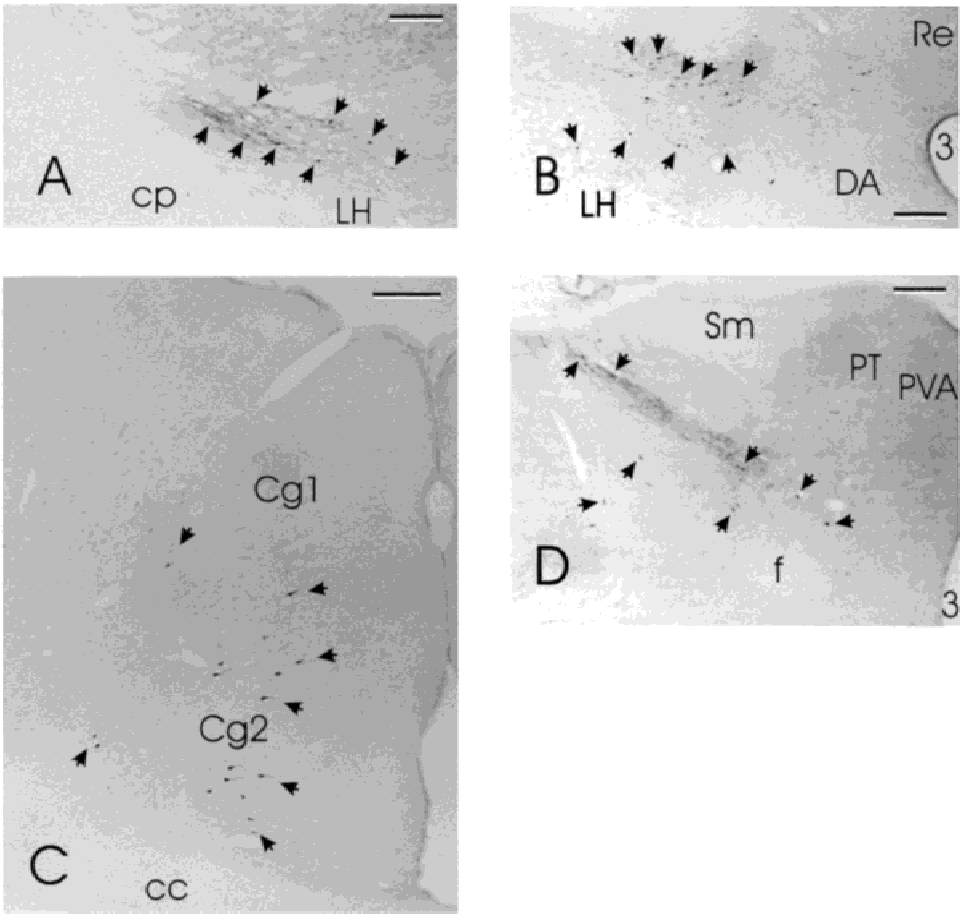

Fig. 7. Photomicrographs of retrogradely labeled neurons in (A) cingulate cortex, (B) bed nucleus of the stria terminalis, posteromedial division, (C) lateral zona incerta, and (D) medial zona incerta after a CT-β injection into the IGL. Scale bar = 200 μm.

Forebrain retinal projections

A small, superficial pathway passes contralaterally through the piriform cortex to a location near the rhinal fissure. It persists in close proximity to the rhinal fissure for a substantial distance caudally into perirhinal cortex (Fig. 8A). A pathway adjacent to the rhinal fissure (Figs. 8B and 8C) also extends rostrally, eventually extending along the base of the fissure medially between olfactory bulb and orbital cortex. The rostral and caudal projections, as typically observed, were substantially less robust than illustrated by this particular case.

Retinal fibers with terminals are visible in rostral hypothalamus. There are numerous bilateral projections to the rostroventral preoptic region (Fig. 9A), particularly in the anteroventrolateral preoptic nucleus, extending laterally into the olfactory tubercle and piriform cortex. Numerous retinal fibers innervate the basal portions of several amygdaloid nuclei (Fig. 9B). Fibers do not appear to reach these areas ipsilateral to the injected eye.

A small, bilateral fiber bundle departs from the dorsal optic tract adjacent to the dorsal lateral geniculate nucleus (DLG) and extends rostrally as a small profile, but dense, superficial terminal plexus (Fig. 10). The final terminal location is ventrolateral to the stria medullaris in the bed nucleus of the stria terminalis, posteromedial division (Fig. 9A). Caudal to the anteroventrolateral preoptic nucleus, innervation is evident bilaterally above the chiasm and is moderately dense in the contralateral ventral medial preoptic area and anteroventrolateral preoptic nucleus. Extremely dense innervation fills the SCN and extends lateral, dorsal, and caudal to the nucleus (Fig. 9B). A fairly substantial bilateral, retinorecipient zone lateral to the SCN includes the adjacent anterior hypothalamus, and extends into the ventral perifornical region and lateral hypothalamus. At the caudal end of this region, a small but distinct set of retinal projections can be seen terminating in the basal lateral hypothalamus contiguous with the optic tract and the plexus continues caudally into tuberal hypothalamus. Also at the caudal end of this region, modest numbers of retinal fibers can be seen innervating the subgeniculate nucleus and dorsolateral zona incerta (not shown). The peri-SCN innervation extends caudally in a dwindling terminal plexus that fills the subparaventricular zone. The caudal subparaventricular retinorecipient plexus merges with a less dense terminal zone in the periventricular and dorsomedial hypothalamic nuclei (Fig. 9C). At this level, a modest terminal plexus is present in the medial zona incerta. A very few visual fibers are found in the paraventricular hypothalamus and dorsally in the thalamic nucleus reuniens. None are visible in other midline thalamic nuclei or in the anterior or posterior paraventricular thalamic nuclei. Fibers also specifically avoid the core region of the ventromedial hypothalamic nucleus.

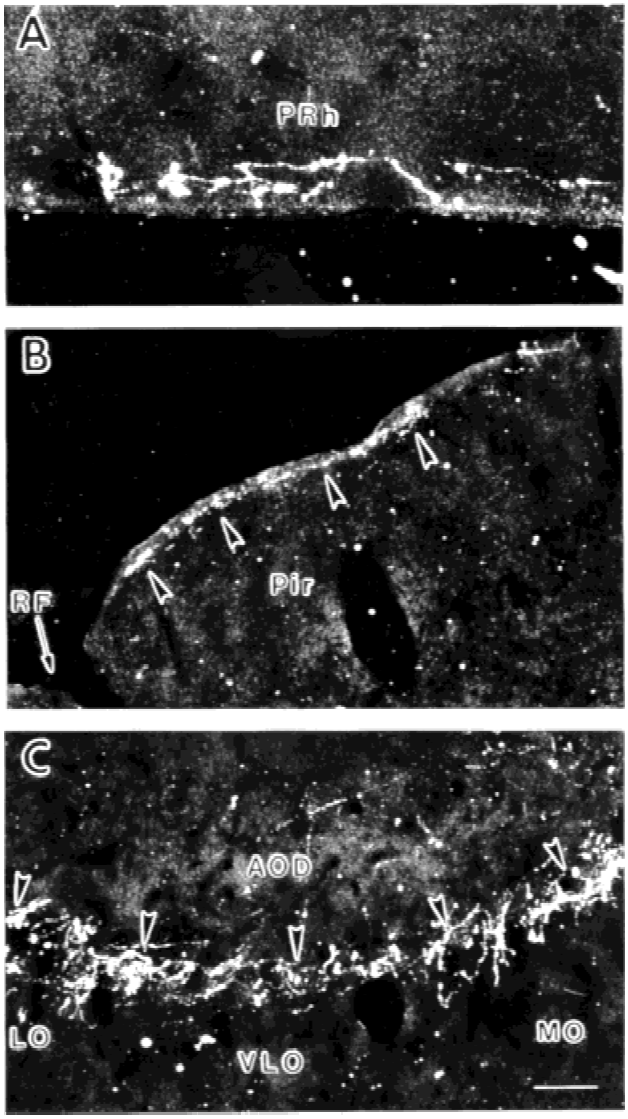

Fig. 8. Dark-field photomicrographs of CT-β-IR retinal projections showing (A) fibers and terminals caudally in superficial perirhinal cortex, (B) fiber segments (arrowheads) rostrally in the lateral olfactory tract, and (C) fibers with terminals (arrowheads) spreading medially along the base of the rhinal fissure between lateral orbital cortex and olfactory bulb. Scale bar = 10 μm for (A) and 20 μm for (B) and (C).

Discussion

The IGL is a major constituent of the subcortical visual system (Morin & Blanchard, 1998). As part of that system, the IGL receives abundant direct retinal projections and has both efferent and afferent connections with virtually all pretectal nuclei and the superior colliculus. The present data demonstrate similar widespread connections between the IGL and certain diencephalic nuclei, particularly within the hypothalamus, and with nuclei in the ventral telencephalon. These are matched by direct retinal projections to the majority of the same regions. As is the case with mesencephalic nuclei of the subcortical visual shell (Morin & Blanchard, 1997), forebrain nuclei with IGL connections seem to have both direct and indirect access to visual signals.

IGL projections to the forebrain

Autoradiographic investigation of rat ventral lateral geniculate projections revealed ample innervation of the hypothalamus (Swanson et al., 1974; Ribak & Peters, 1975), but did not distinguish IGL from VLG as the nucleus of origin. The present extensive IGL projections to hypothalamus in the hamster are similar to what has been described in gerbil (Mikkelsen, 1990) and rat (Moore et al., 1996; Horvath, 1998), also derived from studies using PHAL as the anterograde tracer. In all three species, a major target is an area extending from the lateral optic chiasm medially through the lateroanterior hypothalamus to the midline, including the SCN, and dorsally to include the subparaventricular zone and adjacent perifornical anterior hypothalamus. As in the rat (Horvath, 1998), the

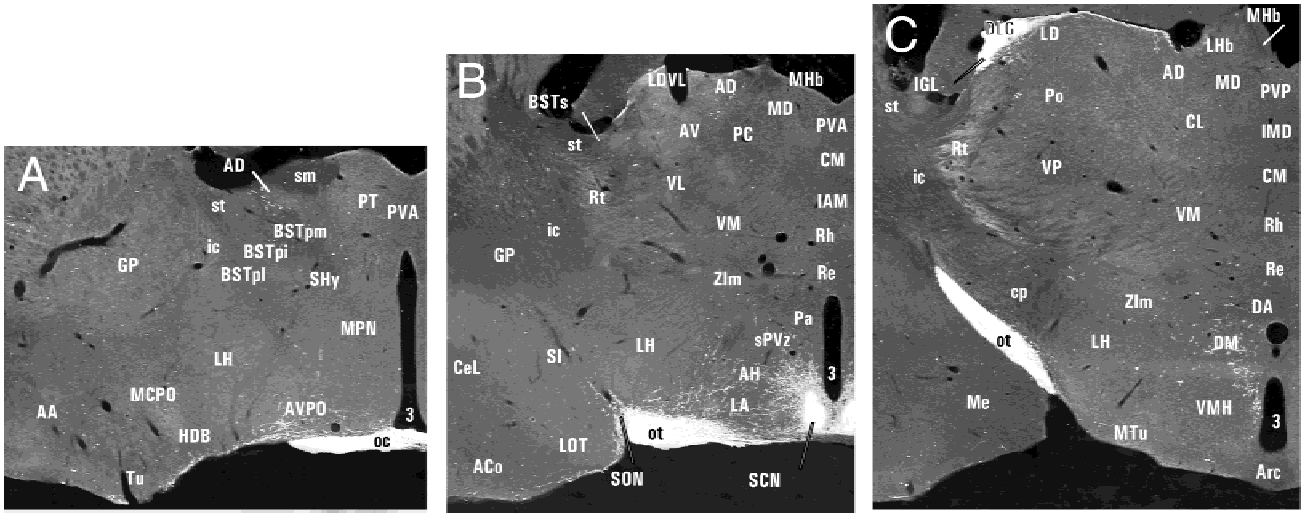

Fig. 9. Dark-field photomicrographs showing retinal ganglion cell projections to hypothalamus and basal telencephalon at (A) rostral, (B) middle, and (C) caudal hypothalamic levels of section. Scale bar = 500 μm.

pattern of hypothalamic innervation by the IGL of the hamster is generally similar to that of SCN efferent projections (Morin et al., 1994) (Table 1).

Projections to the SCN from IGL neurons are dense, as expected (Card & Moore, 1989; Morin & Blanchard, 1995). As suggested previously (Card & Moore, 1989), the SCN may receive innervation from the IGL *via* two or more routes. There is a thin, dense laminar tract on the medial surface of the optic tract that could provide innervation entering ventrally from the supraoptic decussation. A second route to the SCN appears to be *via* projections extending ventromedially across the ventral thalamic nucleus and anterior hypothalamus.

Thalamic projections of the IGL have not been fully characterized, although a dense projection to the contralateral IGL is well documented in rat (Card & Moore, 1989) and hamster (Morin & Blanchard, 1995). The IGL also projects bilaterally to the VLG, but does not innervate the major thalamic visual relay nuclei. However, anterograde tracing methods supported the presence of a projection from the IGL to the intramedullary area of the thalamic lateral posterior nucleus (Morin & Blanchard, 1998). The present study provides retrograde data to affirm this the presence of such a pathway. The intramedullary area is an exception to the rule that thalamic structures projecting to cortex are not innervated by the IGL. As such, it probably should be considered as fully distinct from the lateral posterior nucleus, rather than a subdivision of it.

Several thalamic nuclei located rostromedially, the parataenial, anterior paraventricular, and paracentral, are innervated by IGL projections. These, plus the posterointermediate and posteromedial divisions of the bed nucleus of the stria terminalis, provide avenues for IGL fibers to reach midline thalamic nuclei (central medial, reuniens) where there is a substantial degree of decussation contributing to innervation of contralateral nuclei. IGL projections to the habenula, paraventricular thalamic nucleus (anterior and posterior), and the parataenial nucleus shown here for the hamster have not been previously reported. The thalamic subgeniculate nucleus and zona incerta are also innervated by the IGL with the medial zona incerta, in particular, receiving moderately dense projections in hamster, rat, and gerbil (present data and (Mikkelsen, 1990; Horvath, 1998)).

IGL projections have been noted as far rostral as the medial septum and vertical limb of the diagonal band of Broca in the rat (Horvath, 1998). Innervation of these two regions was sparse in the hamster. Fibers with terminals from the hamster IGL were found in the intermediate lateral septum, anterior divisions of the bed nucleus of the stria terminalis, and the horizontal limb of the diagonal band of Broca. This pattern is consistent with the additional observations that IGL innervation extends rostrolaterally into basal telencephalic regions, including anterior and medial amygdala.

Retinal projections to forebrain

We have previously described four distinct routes of rostral diencephalic retinal innervation in the hamster: (1) the largest, to SCN and the anterior hypothalamic area laterally and caudally; (2) to the ventral lateral hypothalamic area; (3) a rostral projection to ventral preoptic area; and (4) a site in the putative anterodorsal thalamic (Johnson et al., 1988*a*) or bed nucleus of the stria terminalis (Cooper et al., 1994). The present data, obtained with the more sensitive CT-β immunohistochemical method, largely substantiate the previous report, but also add several new observations and reinterpretations.

With respect to the first two pathways, the major difference concerns the density of visual projections to non-SCN hypothalamus. The present data indicate substantially greater innervation than previously reported, particularly in the lateroanterior nucleus, subparaventricular zone, and ventral lateral hypothalamus. Retinal innervation of the paraventricular hypothalamus is very sparse [present data and (Johnson et al., 1988*a*); but see (Cooper et al., 1994)]. The present data also show modestly dense medial hypothalamic innervation extending to the dorsomedial nucleus, a feature not previously reported. It should be emphasized that terminating visual projections are not present in the core of the ventromedial hypothalamic nucleus, but are found dorsally, medially, and ventrally in the "shell" region of the ventromedial hypothalamic nucleus.

The present data also demonstrate retinal innervation of the ventral preoptic area comparable to, although somewhat denser than, previous reports (Johnson et al., 1988*a*). Visual projections

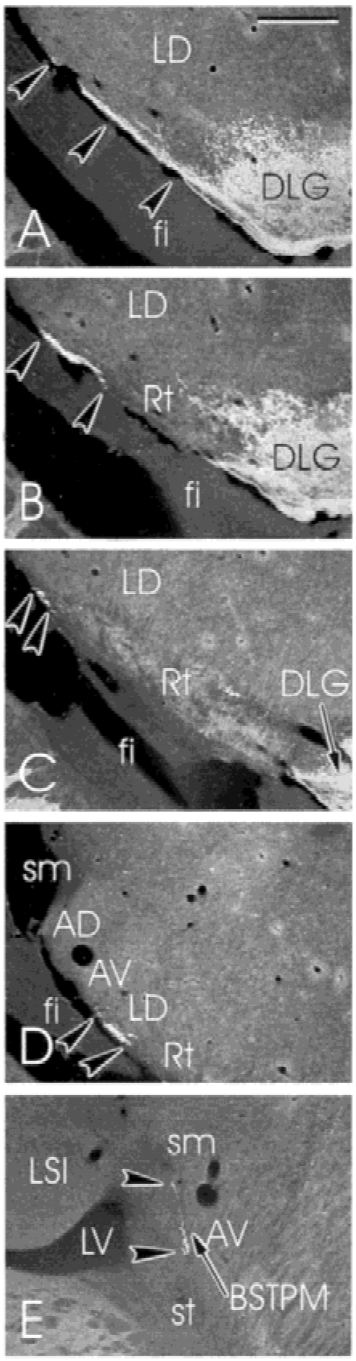

Fig. 10. Dark-field photomicrographs of horizontal sections showing (A) the emergence of a retinal projection rostrally (arrowheads) from the optic tract adjacent to the dorsal lateral geniculate nucleus, and (B–D) extending progressively further rostral, with terminals along the way, finally terminating in a narrow part of the bed nucleus of the stria terminalis, posteromedial division. Scale bar = 500 μm.

through this region extend further laterally into telencephalon. Ventral telencephalic retinal projections have been identified across 13 mammalian orders in 50 species (Cooper et al., 1989, 1994). The present data reveal sparse innervation in anterior and medial amygdaloid nuclei, with most fibers and terminals located superficially, passing ventral to the nucleus of the lateral olfactory tract into layer 1 of the piriform cortex. This is consistent with the original description in the hamster (Pickard & Silverman, 1981), as well as a more recent report (Cooper et al., 1994), although some investigators have not seen this projection in either rat or hamster (Johnson et al., 1988*a*).

An unexpected component of the retinal projection pattern is the presence of a small, but consistent, lateral pathway to the vicinity of the rhinal fissure. The innervation persists caudally, adjacent to the fissure, to the perirhinal cortex. The data also show a similarly small rostral projection into the lateral olfactory tract. The projection extends rostrally in the lateral olfactory tract, eventually curving medially along the ventral surface of the rhinal fissure, beneath overlying frontal cortex.

The fourth retinal pathway has been previously identified as terminating in the anterodorsal thalamic nuclei (Johnson et al., 1988*a*) or "encapsulated" part of the bed nucleus of the stria terminalis (Cooper et al., 1994). Analysis of horizontal sections shows that this retinal projection actually provides a terminal plexus extending a fairly long distance superficially along the lateral surface of the laterodorsal thalamic nucleus. We concur with the view of Cooper and colleagues that the site of final termination of this pathway is in the bed nucleus of the stria terminalis, posterolateral division.

The major thalamic nuclei receiving retinal projections are the VLG, IGL, dorsal lateral geniculate, and lateral posterior nuclei. The present data show sparse innervation of the nucleus reuniens as well. No other thalamic nuclei were consistently identified as receiving retinal projections [present data and (Johnson et al., 1988*a*)], although such projections have been reported in other midline thalamic nuclei, including the anterior paraventricular, and in the anteroventral and anterodorsal nuclei (Cooper et al., 1994).

Forebrain projections to the IGL or VLG

Forebrain afferents of the IGL and VLG have not been widely studied. The present data show that few structures contain neurons projecting to the IGL. The most robust collections of IGL-afferent neurons are found in the posteromedial division of the bed nucleus of the stria terminalis, zona incerta, and subgeniculate nucleus. Smaller numbers are found in the peri-SCN and retrochiasmatic regions [present data and (Morin et al., 1992)]. In the rat, IGL-afferent neurons are found directly in the SCN (Card & Moore, 1989; Vrang & Mikkelsen, 1996). The zona incerta and retrochiasmatic projections to IGL have also been noted in the rat, along with innervation from the ventromedial hypothalamic nucleus (Vrang & Mikkelsen, 1996). The latter is not evident in the hamster (present data). Many more labeled neurons projecting to the IGL or VLG are found dorsally and caudally in mesencephalic nuclei of the pretectum and tectum (Morin & Blanchard, 1998).

The IGL and VLG receive innervation from the posterior cingulate cortex in both rat (Vrang & Mikkelsen, 1996) and hamster (present data). Although both IGL and VLG project to the intramedullary area of the lateral posterior thalamic nucleus [present data and (Morin & Blanchard, 1998)], this area does not reciprocally project to either.

Connections of the VLG

Initial evaluations of VLG projections to the rat hypothalamus were made in the absence of knowledge about the IGL (Ribak & Peters, 1975). The present study employed both anterograde and retrograde methods to determine the extent of VLG projections to

rostral thalamus, hypothalamus, and telencephalon. The PHAL anterograde tracing method indicated that a limited number of nuclei might receive projections from the VLG. CT-β retrograde label confirmed the presence of innervation from the VLG in most of the nuclei containing at least modestly robust projections. If the PHAL-IR material indicated sparse innervation to a particular location (e.g. lateral hypothalamus), then a CT-β injection at that site failed to retrogradely label VLG neurons. The nuclei identified from the PHAL-IR material as receiving modestly robust projections include the bed nucleus of the stria terminalis, central medial thalamic nucleus, and the medial zona incerta. Retrograde analysis also shows a VLG projection to the intramedullary area of the thalamic lateral posterior nucleus in accordance with previous anterograde data (Morin & Blanchard, 1998). All diencephalic nuclei receiving VLG projections are fairly dorsal and none is hypothalamic, a feature consistent with previous reports in rat (Horvath, 1998) and gerbil (Mikkelsen, 1990). Thus, it is likely that the limited immunoreactive fibers and terminals seen in the basal hypothalamus after a VLG injection of PHAL are consequent to label leakage into adjacent IGL. The VLG and IGL do not differ greatly with respect to the specific nuclei of the subcortical visual shell to which they are connected. However, one clear trait of the IGL is the presence of bilaterally efferent projections (although it is not known whether individual neurons project bilaterally). This is evident both with respect to projections to nuclei of the subcortical visual shell (Morin & Blanchard, 1998) and with respect to more rostral projections (present data). We previously demonstrated that IGL, but not VLG, neurons project to SCN (Morin & Blanchard, 1995). The present data generalize this observation by showing that lateral geniculate neurons projecting to hypothalamus are found only in the IGL.

Functional considerations

The visual system has typically been partitioned into two major divisions, one concerned with sophisticated image analysis and another concerned with oculomotor control. The circadian visual system has been described as a third division of the overall visual plan (Morin, 1994). The two major nuclei of this system are the SCN and IGL. Briefly, the SCN receives a direct retinal projection that transmits photic information necessary for entrainment to the circadian clock in that nucleus (Johnson et al., 1988*a*,*b*; Ding et al., 1994). The IGL also receives a direct retinal projection and can provide indirect photic information to the SCN (Zhang & Rusak, 1989). The IGL is not necessary for rhythm generation or photic entrainment, but can modulate the effects of light on rhythmicity (Harrington & Rusak, 1986; Pickard et al., 1987; Johnson et al., 1989). The IGL is necessary for circadian rhythm phase control by several nonphotic stimuli (Johnson et al., 1988*c*; Biello et al., 1991; Wickland & Turek, 1994; Janik & Mrosovsky, 1994).

As a rule, the IGL does not connect with thalamic relay nuclei involved with complex visual image analysis (Morin & Blanchard, 1998). The intramedullary area of the lateral posterior nucleus, situated ventrolaterally adjacent to the DLG, is a noteworthy exception to this rule. Its neurons project to secondary visual cortex area 18a (Takahashi, 1985; Morin & Blanchard, 1998) which may be involved in pattern discrimination (Dean, 1981). The IGL has extensive interconnections with all subcortical visual nuclei participating in various forms of oculomotor control (see Morin & Blanchard, 1998 for a discussion). Thus, the circadian visual system is not fully separable from the two major divisions of the visual system. At the moment, it is not possible to state the function of the rather extensive relationship between cortical or subcortical visual nuclei and the IGL.

The IGL appears to have similarly extensive connections with forebrain nuclei not customarily thought to have visual function. There is no direct information from the hamster concerning function of second-order visual information conveyed to non-SCN, non-geniculate forebrain structures *via* the IGL. However, data from the rat indicate that retinal fibers terminate on IGL neurons projecting to non-SCN hypothalamus and that tonic photic stimulation may act through the IGL to regulate certain endocrine functions in rats (Horvath, 1998). Putative neuroendocrine targets of IGL projections are dopamine neurons in the rat ventral medial hypothalamus. The present data show a direct retinal projection to the same region, suggesting redundancy between direct and indirect (i.e. from IGL) retinal projections. A similar phenomenon has been demonstrated in the mesencephalic nuclei of the subcortical visual shell to the extent that all receive both direct retinal projections and projections from the IGL (Morin & Blanchard, 1997, 1998).

Horvath (1998) has emphasized another form of apparent visual projection redundancy in his description of similar hypothalamic innervation patterns independently arising from IGL and SCN neurons. Similarity of innervation is a theme also discussed by Cooper and colleagues (Cooper et al., 1994) who have indicated that olfaction-related projections to hypothalamus and direct retinal projections often innervate common areas. However, there is very little evidence to support any function of direct retinal input related to olfaction-mediated physiology or behavior. Neither is there much data supporting the possibility of physiological or behavioral regulation by either direct, non-SCN, retinohypothalamic innervation, or indirect innervation from the IGL. The non-SCN, direct, and indirect visual projections to hypothalamus could be involved in circadian rhythm "masking." Masking effects are seen when a stimulus induces increased or decreased amplitude of a rhythmic variable (e.g. number of daily wheel revolutions) rather than through a change in phase or period of the pacemaker system regulating the timing of that variable. In the rat, the acoustic startle response is amplified by a concomitant bright light (Walker & Davis, 1997). This effect is blocked by lesions of the bed nucleus of the stria terminalis. It is possible that the visual projection described here as innervating the nearby border of stria medullaris and anterodorsal thalamic nucleus contributes to that response facilitation. However, our previous study of retinal forebrain projections did not identify such a pathway in rat (Johnson et al., 1988*b*).

The mechanism generating circadian rhythmicity normally provides an oscillatory substrate modulating the likelihood of sleep (Borbely, 1975; Ibuka & Kawamura, 1975). However, light can have direct effects on this and other behaviors in addition to indirect actions through circadian clock regulation. For example, lights OFF will acutely induce rapid-eye-movement (REM) sleep (Lisk & Sawyer, 1966) and is associated with reduced slow wave sleep (Borbely, 1975). Lights ON will acutely inhibit waking, feeding, drinking, and locomotion (Borbely & Huston, 1974; Borbely et al., 1975). The acute effects of lights off on REM sleep may be mediated through pretectal nuclei (Miller et al., 1997). Whether the acute effects of light or dark on feeding, drinking, and locomotion are also mediated through pretectal nuclei or are simultaneously elicited through direct or indirect photic input to hypothalamus have not yet been studied.

In summary, the present data show widespread projections of the IGL to the forebrain, especially the hypothalamus. Both olfactory and retinal projections appear to project to many of the same

regions. The pattern of ascending IGL projections is easily distinguishable from that contributed by VLG neurons. Through its extensive projections to both forebrain and midbrain, the IGL appears to have the capacity, largely untested at this time, to modulate numerous aspects of normal physiology and behavior.

Acknowledgments

This research was supported by NIH NINDS Grant NS22168.

References

Biello, S.M., Harrington, M.E. & Mason, R. (1991). Geniculo-hypothalamic tract lesions block chlordiazepoxide-induced phase advances in Syrian hamsters. *Brain Research* **552**, 47–52.

Borbely, A.A. (1975). Circadian rhythm of vigilance in rats: Modulation by short light–dark cycles. *Neuroscience Letters* **1**, 67–71.

Borbely, A.A. & Huston, J.P. (1974). Effects of two-hour light–dark cycles on feeding, drinking and motor activity of the rat. *Physiology and Behavior* **13**, 795–802.

Borbely, A.A., Huston, J.P. & Waser, P.G. (1975). Control of sleep states in the rat by short light–dark cycles. *Brain Research* **95**, 89–101.

Card, J.P. & Moore, R.Y. (1989). Organization of lateral geniculate-hypothalamic connections in the rat. *Journal of Comparative Neurology* **284**, 135–147.

Coolen, L.M. & Wood, R.I. (1998). Bidirectional connections of the medial amygdaloid nucleus in the syrian hamster brain: Simultaneous anterograde and retrograde tract tracing. *Journal of Comparative Neurology* **399**, 189–209.

Cooper, H.M., Mick, G. & Magnin, M. (1989). Retinal projection to mammalian telencephalon. *Brain Research* **477**, 350–357.

Cooper, H.M., Parvopassu, F., Herbin, M. & Magnin, M. (1994). Neuroanatomical pathways linking vision and olfaction in mammals. *Psychoneuroendocrinology* **19**, 623–639.

Dean, P. (1981). Grating detection and visual acuity after lesions of striate cortex in hooded rats. *Experimental Brain Research* **43**, 145–153.

Ding, J.M., Chen, D., Weber, E.T., Faiman, L.E., Rea, M.A. & Gillette, M.U. (1994). Resetting the biological clock: Mediation of nocturnal circadian shifts by glutamate and NO. *Science* **266**, 1713–1717.

Harrington, M.E., Nance, D.M. & Rusak, B. (1985). Neuropeptide Y immunoreactivity in the hamster geniculo-suprachiasmatic tract. *Brain Research Bulletin* **15**, 465–472.

Harrington, M.E. & Rusak, B. (1986). Lesions of the thalamic intergeniculate leaflet alter hamster circadian rhythms. *Journal of Biological Rhythms* **1**, 309–325.

Hickey, T.L. & Spear, P.D. (1976). Retinogeniculate projections in hooded and albino rats: An autoradiographic study. *Experimental Brain Research* **24**, 523–529.

Horvath, T.L. (1996). Evidence that circadian and visual signals from the SCN and LGN are integrated on neuroendocrine dopamine cells in the rat hypothalamus. *Society for Neuroscience* **26**, 31.

Horvath, T.L. (1997). Suprachiasmatic efferents avoid phenestrated capillaries but innervate neuroendocrine cells, including those producing dopamine. *Endocrinology* **138**, 1312–1320.

Horvath, T.L. (1998). An alternate pathway for visual signal integration into the hypothalamo-pituitary axis: Retinorecipient intergeniculate neurons project to various regions of the hypothalamus and innervate neuroendocrine cells including those producing dopamine. *Journal of Neuroscience* **18**, 1546–1558.

Hsu, S.-M., Raine, L. & Fanger, H. (1981). Use of avidin-biotin-perioxidase complex (ABC) in immunoperioxidase techniques: A comparison between ABC and unlabeled antibody (PAP) procedures. *Journal of Histochemistry and Cytochemistry* **29**, 577–580.

Ibuka, N. & Kawamura, H. (1975). Loss of circadian rhythm in sleep-wakefulness cycle in the rat by suprachiasmatic nucleus lesions. *Brain Research* **96**, 76–81.

Janik, D. & Mrosovsky, N. (1994). Intergeniculate leaflet lesions and behaviorally-induced shifts of circadian rhythms. *Brain Research* **651**, 174–182.

Johnson, R.F., Moore, R.Y. & Morin, L.P. (1988*a*). Loss of entrainment and anatomical plasticity after lesions of the hamster retinohypothalamic tract. *Brain Research* **460**, 297–313.

Johnson, R.F., Morin, L.P. & Moore, R.Y. (1988*b*). Retinohypothalamic projections in the hamster and rat demonstrated using cholera toxin. *Brain Research* **462**, 301–312.

Johnson, R.F., Smale, L., Moore, R.Y. & Morin, L.P. (1988*c*). Lateral geniculate lesions block circadian phase shift responses to a benzodiazepine. *Proceedings of the National Academy of Sciences of the U.S.A.* **85**, 5301–5304.

Johnson, R.F., Moore, R.Y. & Morin, L.P. (1989). Lateral geniculate lesions alter activity rhythms in the hamster. *Brain Research Bulletin* **22**, 411–422.

Klein, D.C., Moore, R.Y. & Reppert, S.M. (1991). *Suprachiasmatic Nucleus: The Mind's Clock.* New York: Oxford University Press.

Lisk, R.D. & Sawyer, C.H. (1966). Induction of paradoxical sleep by lights-off stimulation. *Proceedings of the Society for Experimental Biology and Medicine* **123**, 664–667.

McLean, I.W. & Nakane, P.K. (1974). Periodate-lysine-paraformaldehyde fixative: A new fixative for immunoelectron microscopy. *Journal of Histochemistry and Cytochemistry* **22**, 1077–1083.

Mikkelsen, J.D. (1990). Projections from the lateral geniculate nucleus to the hypothalamus of the Mongolian gerbil (*Meriones unguiculatus*): An anterograde and retrograde tracing study. *Journal of Comparative Neurology* **299**, 493–508.

Miller, A.M., Oblinger, M.M., Behan, M. & Benca, R.M. (1997). Ibotenic acid lesions of the pretectum affect REM triggering, but not redistribution of sleep in short light–dark cycles. *Society for Neuroscience* **23**, 2132.

Moore, R.Y. & Card, J.P. (1994). Intergeniculate leaflet: An anatomically and functionally distinct subdivision of the lateral geniculate complex. *Journal of Comparative Neurology* **344**, 403–430.

Moore, R.Y., Moga, M.M. & Weis, R. (1996). Intergeniculate leaflet and ventral lateral geniculate projections in the rat. *Society for Neuroscience* **26**, 31.

Moore, R.Y. & Speh, J.C. (1993). GABA is the principal neurotransmitter of the circadian system. *Neuroscience Letters* **150**, 112–116.

Morin, L.P. (1994). The circadian visual system. *Brain Research Review* **67**, 102–127.

Morin, L.P. & Blanchard, J.H. (1995). Organization of the hamster intergeniculate leaflet: NPY and ENK projections to the suprachiasmatic nucleus, intergeniculate leaflet and posterior limitans nucleus. *Visual Neuroscience* **12**, 57–67.

Morin, L.P. & Blanchard, J.H. (1997). Neuropeptide Y and enkephalin immunoreactivity in retinorecipient nuclei of the hamster pretectum and thalamus. *Visual Neuroscience* **14**, 765–777.

Morin, L.P. & Blanchard, J.H. (1998). Interconnections among nuclei of the subcortical visual shell: The intergeniculate leaflet is a major constituent of the hamster subcortical visual system. *Journal of Comparative Neurology* **396**, 288–309.

Morin, L.P., Blanchard, J.H. & Moore, R.Y. (1992). Intergeniculate leaflet and suprachiasmatic nucleus organization and connections in the hamster. *Visual Neuroscience* **8**, 219–230.

Morin, L.P., Goodless-Sanchez, N., Smale, L. & Moore, R.Y. (1994). Projections of the suprachiasmatic nuclei, subparaventricular zone and retrochiasmatic area in the golden hamster. *Neuroscience* **61**, 391–410.

Pickard, G.E., Ralph, M.R. & Menaker, M. (1987). The intergeniculate leaflet partially mediates effects of light on circadian rhythms. *Journal of Biological Rhythms* **2**, 35–56.

Pickard, G.E. & Silverman, A.J. (1981). Direct retinal projections to hypothalamus, piriform cortex and accessory optic nuclei in the golden hamster as demonstrated by a sensitive anterograde horseradish peroxidase technique. *Journal of Comparative Neurology* **196**, 155–172.

Ribak, C.E. & Peters, A. (1975). An autoradiographic study of the projections from the lateral geniculate body of the rat. *Brain Research* **92**, 341–368.

Swanson, L.W., Cowan, W.M. & Jones, E.G. (1974). An autoradiographic study of the efferent projections of the ventral lateral geniculate nucleus in the albino rat and cat. *Journal of Comparative Neurology* **156**, 143–164.

Takahashi, T. (1985). The organization of the lateral thalamus of the hooded rat. *Journal of Comparative Neurology* **231**, 281–309.

Taylor, A.M., Jeffery, G. & Lieberman, A.R. (1986). Subcortical afferent and efferent connections of the superior colliculus in the rat and comparisons between albino and pigmented strains. *Experimental Brain Research* **62**, 131–142.

VRANG, N. & MIKKELSEN, J.D. (1996). Afferent connections of the intergeniculate leaflet of the golden hamster: A combined retrograde and anterograde tracing study. *Society for Neuroscience* **26**, 232.

WALKER, D.L. & DAVIS, M. (1997). Double dissociation between the involvement of the bed nucleus of the stria terminalis and the central nucleus of the amygdala in startle increases produced by conditioned versus unconditioned fear. *Journal of Neuroscience* **17**, 9375–9383.

WATTS, A.G., SWANSON, L.W. & SANCHEZ-WATTS, G. (1987). Efferent projections of the suprachiasmatic nucleus: I. Studies using anterograde transport of Phaseolus vulgaris leucoagglutinin in the rat. *Journal of Comparative Neurology* **258**, 204–229.

WICKLAND, C. & TUREK, F.W. (1994). Lesions of the thalamic intergeniculate leaflet block activity-induced phase shifts in the circadian activity rhythm of the golden hamster. *Brain Research* **660**, 293–300.

ZHANG, D.X. & RUSAK, B. (1989). Photic sensitivity of geniculate neurons that project to the suprachiasmatic nuclei or the contralateral geniculate. *Brain Research* **504**, 161–164.